University of Groningen

Lagrangian Modeling and Control of Switching Networks with Integrated Coupled Magnetics

Scherpen, Jacquelien M.A.; Jeltsema, Dimitri; Klaassens, J. Ben

[Link to publication in University of Groningen/UMCG research database](#)

Lagrangian Modeling and Control of Switching Networks with Integrated Coupled Magnetics

Jacquelien M.A. Scherpen, Dimitri Jeltsema, J. Ben Klaassens

Fac. ITS, Dept. of Electrical Eng., Delft University of Technology,
P.O. Box 5031, 2600 GA Delft, The Netherlands.
E-mail: j.m.a.scherpen/d.jeltsema/j.b.klaassens@its.tudelft.nl
Phone: +31-15-278/-6152/-4516/-2928, Fax: +31-15-278-6679

Abstract - In this paper a method is presented to build an Euler-Lagrange model for electrical networks, including switches and integrated (non-ideal) coupled-magnetics, in a structured general way. One of the advantages of emphasizing the physical structure of these systems is its functionality during the controller design stage. In case a switching network contains coupled-inductor structures, an additional path for the energy transfer is introduced. For this reason, a basic building block is proposed that describes the dynamical behaviour of a pair of magnetically coupled-inductors. This building block is applicable to all types of switching converters, and easily predicts the existence of reduced or zero-ripple current. The switches make the dynamic models nonlinear. For using the Lagrangian structure for controller design, the zero-dynamics for such switching network had to be studied. It is shown that under certain coupling conditions it will not be possible to design a globally stable controller. The approach is illustrated by means of the coupled-inductor Ćuk-converter with zero-output ripple, in closed loop with an adaptive passivity-based controller.

1 Introduction

During the last thirty years major research has been devoted to optimization of modeling, design and control techniques of DC-to-DC switched-mode power converters. In recent developments these systems are considered from a physical modeling point of view. It is shown in [9, 11] that the conventional average PWM (pulse width modulation) models of the classical Buck, Boost, Buck-Boost and the more complex Ćuk converter correspond to systems derived from classical Euler-Lagrange (or Hamiltonian, [2]) dynamic considerations. The approach consists of establishing a suitable set of average *Euler-Lagrange (EL) parameters* modulated by the duty ratio function. Here, we develop a procedure that results in the EL parameters of a general switching electrical network structure, where we assume switches to be ON and OFF, and where the EL parameters are extended with constraint equations stemming from Kirchhoff's current laws. The major advantage of emphasizing the physical structure of the systems is its functionality during the controller design stage. This will finally lead to feedback (passivity-based) controlled systems that do not involve cancellation of non-linearities and are globally defined, see e.g. [6, 10].

The Lagrangian approach for switching networks as initiated in [9, 11] was up to now, build on the assumption that the converters, and electrical circuits in general, do not contain any magnetic couplings between its different loops. Here, this assumption is no longer necessary, since we include essential terms that correspond to the magnetic energy of the coupling into the Lagrangian description.

As shown in [9, 11], the non-minimum phase character of the converters above induces several difficulties for the application of passivity-based control techniques. For this reason, the output is controlled indirectly through the regulation of the input current. We can show that there exists a range of coupling 'mismatch' adjustments for which all currents and voltages show unstable zero-dynamics. This is mainly caused by the additional magnetic coupling between the loops in the network. In this case it is not possible to design a globally stable controller. In addition we show that for exact matching conditions (zero-current ripple) the order of the zero-dynamics is reduced.

In Section 2 we present the general procedure to develop an EL model for switching and non-switching electrical networks. Then, in Section 3 we show how to include coupled-magnetics into the EL model. Section 4 treats a study of the stability of the zero-dynamics, corresponding to the (non-) minimum phase behaviour of the output in relation to the coupling adjustments. In Section 5 an adaptive passivity-based controller for the Ćuk converter with zero-output ripple is developed. Simulations are presented. Finally, in Section 6 we end with the conclusions and recommendations.

2 Euler-Lagrange Modeling of Electrical (Switching) Networks

The constraint EL dynamics of an electrical circuit Σ_e can in general be characterized as follows [11]:

$$\Sigma_e : \quad \frac{d}{dt}\left(\frac{\partial \mathcal{L}}{\partial \dot{q}}\right) - \frac{\partial \mathcal{L}}{\partial q} = -\frac{\partial \mathcal{D}}{\partial \dot{q}} + A(q)\lambda + \mathcal{F}_q \quad (1)$$
$$A(q)^\top \dot{q} = 0$$

where $\dot{q}$ is the vector of flowing *current* and q represents the electric *charge*. The vector q constitutes the *generalized coordinates* describing the circuit and is assumed to have N components, represented by $q_1, \ldots, q_N$. It is well-known that the scalar function $\mathcal{L}$ is the *Lagrangian* of the system, defined as the difference between the *magnetic co-energy* of the circuit, denoted by $T(q, \dot{q})$, and the *electric field energy* of the circuit, denoted by $V(q)$, i.e., $\mathcal{L}(q, \dot{q}) = T(q, \dot{q}) - V(q)$. The function $\mathcal{D}(\dot{q})$ is the *Rayleigh dissipation cofunction* of the system. The vector $\mathcal{F}_q = [\mathcal{F}_{q_1}, \ldots, \mathcal{F}_{q_N}]$ represents the ordered components of the set of *generalized forcing functions*, or voltage sources, associated with each generalized coordinate. The

constraints that follow from Kirchhoff's current laws are captured in $A(q)$. Following ([6]), we refer to the set of functions $(\mathcal{T}, \mathcal{V}, \mathcal{D}, \mathcal{F}_q)$ as the *EL parameters* of the circuits, and simply express a circuit Σ_e by means of the ordered five-tuple:

$$\Sigma_e = (\mathcal{T}, \mathcal{V}, \mathcal{D}, \mathcal{F}_q, A(q)). \qquad (2)$$

The EL equations actually form a balance of generalized forces, or efforts, which in the electrical domain is given by the voltages. It involves both generalized position and generalized velocity coordinates for each separate physical element. In the electrical domain that means that we attach to each separate element (inductor and capacitor) *two* state-variables, namely a charge and a current. Clearly this does not correspond to the physical intuition, but it can be viewed as if for the inductor the charge is an *intermediate help* variable, and for the capacitor the current is. These help variables are finally removed using the constraint equation.

This framework can be used to model electrical networks with linear inductive and capacitive elements and with or without ideal switches. The switches can be naturally involved in the constraints that follow from Kirchhoff's current laws. If we denote by the scalar u the switch position, which is assumed to take values on a discrete set of the form $\{0, 1\}$. The complete procedure is as follows:

Procedure:

1. Give all N dynamic elements in the network two coordinates, namely a charge and a current coordinate, q_j, and $\dot{q}_j, j = 1 \ldots N$.

2. Determine the corresponding energy for all ideal elements, i.e., the magnetic co-energy for the inductive elements, denoted by $\mathcal{T}(q, \dot{q})$, and the electric field energy for the capacitive elements, denoted by $\mathcal{V}(\dot{q})$. In case of a switching network, this step does *not* involve the position of the switch.

3. Determine the Rayleigh dissipation energy, denoted by $\mathcal{D}(\dot{q})$, for the resistive elements, which may involve the switch position u, and the use of a Kirchhoff current law for determining the current through the resistive element in terms of the dynamic elements as given in step 1.

4. Determine the generalized forcing functions $\mathcal{F}_q$ given by the voltage sources, possibly depending on the switch position.

5. Give the constraint equations that are determined by Kirchhoff's currents laws, that do not include the laws of step 3, and thus only involve the currents through the dynamic elements. If there are no constraint equations for this step, then put $A(q) = 0$.

6. Plug the information of the previous steps in the constraint form of the EL equations (1) and determine a state space model by choosing the currents corresponding with the inductive elements, and either the charge or the voltage corresponding with the capacitive elements, as state variables.

The above procedure, as well as the developments in e.g. [9], was initially build upon the assumption that the electric circuits do not contain any magnetic couplings between its different loops. In the following section, we will show that this assumption is no longer necessary.

3 Coupled-Magnetics

In this section we treat the inclusion of coupled-magnetics in the EL framework. First, a pair of magnetically coupled-inductors is considered. Next, we generalize our developments to circuits containing several magnetic couplings between its different loops. As an example, we illustrate the potential of the method using the well-known Ćuk converter in which both the inductors are coupled, e.g. [1].

A pair of coupled-inductors may be considered as the non-ideal equivalent of an AC transformer, with a *rate of coupling*, $k \in [0, 1)$ and an *effective turns ratio* $n = \sqrt{L_1 L_2}$. As a result of the coupling, both the magnetizing currents share the same flux paths with an order or magnitude depending on k. This involves an additional path for the energy using a magnetic field. In terms of the common fluxes ϕ_i, $j = 1, 2$, a pair of coupled-inductors can be characterized as follows

$$\begin{bmatrix} \phi_1 \\ \phi_2 \end{bmatrix} = \begin{bmatrix} L_1 & L_{12} \\ L_{21} & L_2 \end{bmatrix} \begin{bmatrix} i_{L_1} \\ i_{L_2} \end{bmatrix}, \qquad (3)$$

for which $L_{12} \geq 0$ and $L_{21} \geq 0$ satisfy the condition of *reciprocity*, i.e., $L_{12} = L_{21} = L_m = k\sqrt{L_1 L_2}$ denoted as the *mutual* inductance.
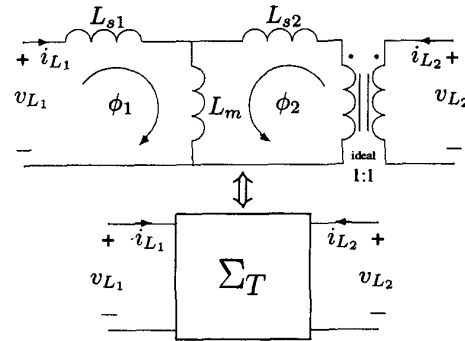
Figure 1: Equivalent topology of a pair of coupled-inductors

¿From these relations it is clear that L_1 and L_2 would form two separate inductors if $k = 0$, and thus $L_m = 0$. For non-zero values of k, L_m is representative for the interaction between the inductors. Now, in order to obtain expressions for the currents and voltages, equation (3) is rewritten as

$$\frac{d}{dt} \begin{bmatrix} i_{L_1} \\ i_{L_2} \end{bmatrix} = \begin{bmatrix} \beta & -\gamma \\ -\gamma & \alpha \end{bmatrix} \begin{bmatrix} v_{L_1} \\ v_{L_2} \end{bmatrix}, \qquad (4)$$

where $v_{L_j} = \frac{d\phi_j}{dt}, j = 1, 2$ and α, β and γ may be expressed as

$$\alpha = \frac{n^2}{(1-k^2)L_1}; \beta = \frac{1}{(1-k^2)L_1}; \gamma = \frac{nk}{(1-k^2)L_1}. \qquad (5)$$

The term $1 - k^2$ can be considered as the magnetic *flux dispersal*, which denotes the amount of flux not shared by both the inductors. Notice that other parameterizations of (5) are also possible but, as will be illustrated later in the example, these notations provide a straightforward insight in the magnetizing energy interconnections. A visual representation of (3) and (4) may be given as in Fig. 1, in which $L_{s_j} = L_j - L_m$ are the leakage inductances of the primary and the secondary winding, respectively. In view of the Lagrangian modeling procedure, we consider a pair of magnetically coupled inductors as a single system Σ_T for which the total amount of stored energy T in terms of the currents is, using (3), given by

$$T(i_{L_1}, i_{L_2}) = \frac{1}{2} \begin{bmatrix} i_{L_1} \\ i_{L_2} \end{bmatrix}^T \begin{bmatrix} L_1 & L_m \\ L_m & L_2 \end{bmatrix} \begin{bmatrix} i_{L_1} \\ i_{L_2} \end{bmatrix}. \quad (6)$$

For general descriptions of the magnetic energy of an electrical network containing N inductors with N magnetically coupled loops, it follows in a similar way that

$$T(q, \dot{q}) = \frac{1}{2} \dot{q}^T \begin{bmatrix} L_1 & L_{12} & \cdots & L_{1N} \\ L_{21} & L_2 & \cdots & L_{2N} \\ \vdots & \vdots & \ddots & \vdots \\ L_{N1} & L_{N2} & \cdots & L_N \end{bmatrix} \dot{q}, \quad (7)$$

where i is subsequently replaced by its generalized coordinates $\dot{q} = [\dot{q}_1, \ldots, \dot{q}_N]^T$. Notice that $T(q, \dot{q})$ satisfies $T(q, \dot{q}) \geq 0$. The separate inductors are denoted by $L_1, \ldots, L_N$, while the mutual inductances $L_{12}, L_{21}, \ldots, L_{N-1,N}, L_{N,N-1}$, denote the various coupling paths between these inductors. If, for example, there exists no coupling between the $M - 1^{th}$ and the Mth inductor the corresponding coefficients are set to zero. As before, notice that in case of a symmetrical network the condition of reciprocity is satisfied.

Example: Coupled-inductor Ćuk converter
This example illustrates the potential of the proposed procedure for switching networks, including coupled-magnetics. We use the coupled-inductor Ćuk converter, which serves as a case study throughout the paper. We explicitly assume that the converter operates at continues conduction mode.
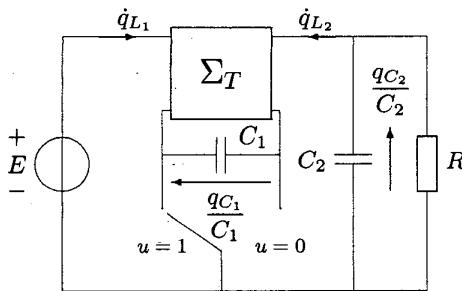

Figure 2: Coupled-inductor Ćuk converter

The circuit topology of the coupled-inductor Ćuk converter is depicted in Fig. 2. The capacitive energy transfer imposes identical rectangular voltage waveforms on both the inductors which has justified the magnetic extension, [1]. Providing the right adjustments of k and n, the input current ripple can

be steered into the output inductor, or vice-versa, to result in practically zero ripple current on either the input or the output of the converter. Following the general procedure as given in section 2, we start with defining the following (intermediate) state variables $q_j, \dot{q}_j$, $j = L_1, C_1, L_2, C_2$. We proceed with equating the magnetic co-energy, $T(q, \dot{q})$, and potential energy, $\mathcal{V}(q)$, of the circuit

$$T(\dot{q}_{L_1}, \dot{q}_{L_2}) = \frac{1}{2} L_1 \dot{q}_{L_1}^2 + \frac{1}{2} L_2 \dot{q}_{L_2}^2 + L_m \dot{q}_{L_1} \dot{q}_{L_2};$$

$$\mathcal{V}(q_{C_1}, q_{C_2}) = \frac{1}{2C_1} q_{C_1}^2 + \frac{1}{2C_2} q_{C_2}^2. \quad (8)$$

The remaining EL properties are readily found to be

$$\mathcal{D}(\dot{q}_{L_2}, \dot{q}_{C_2}) = \frac{1}{2} R(-\dot{q}_{L_2} - \dot{q}_{C_2})^2;$$

$$\mathcal{F}_{q_{L_1}} = E; \quad \mathcal{F}_{q_{C_1}} = \mathcal{F}_{q_{L_2}} = \mathcal{F}_{q_{C_2}} = 0; \quad (9)$$

$$A(q)^T \dot{q} = \dot{q}_{C_1} + u\dot{q}_{L_2} - (1 - u)\dot{q}_{L_1} = 0.$$

Plugging (8) and (9) into the constraint equation (1) yields for the coupled-inductor Ćuk converter:

$$\begin{array}{rcl}
L_1 \ddot{q}_{L_1} + L_m \ddot{q}_{L_2} &=& -(1 - u)\lambda + E \\
\frac{1}{C_1} q_{C_1} &=& \lambda \\
L_2 \ddot{q}_{L_2} + L_m \ddot{q}_{L_1} &=& R(-\dot{q}_{L_2} - \dot{q}_{C_2}) + u\lambda \\
\frac{1}{C_2} q_{C_2} &=& R(-\dot{q}_{L_2} - \dot{q}_{C_2}) \\
0 &=& \dot{q}_{C_1} + u\dot{q}_{L_2} - (1 - u)\dot{q}_{L_1},
\end{array} \quad (10)$$

which results in the state equations for $x = [x_1, x_2, x_3, x_4]^T = [\dot{q}_{L_1}, C_1^{-1} q_{C_1}, \dot{q}_{L_1}, C_2^{-1} q_{C_2}]^T$, in terms of α, β and γ as

$$\begin{array}{rcl}
\dot{x}_1 &=& -u\gamma x_2 - (1 - u)\beta x_2 - \gamma x_4 + \beta E \\
\dot{x}_2 &=& (1 - u)\frac{1}{C_1} x_1 - u\frac{1}{C_1} x_3 \\
\dot{x}_3 &=& u\alpha x_2 + (1 - u)\gamma x_2 + \alpha x_4 - \gamma E \\
\dot{x}_4 &=& -\frac{1}{C_2} x_3 - \frac{1}{RC_2} x_4.
\end{array} \quad (11)$$

This is the model with discrete values for the switch, where x_1, x_3 represent the inductor currents, and x_2, x_4 represent the capacitor voltages. We have thus shown that the assumptions in e.g. [11] and [9] are no longer necessary. With help from the definitions in (5) it is now easy to see that for the *matching condition*, $n = k$, $\alpha = \gamma$, the state x_3 does not depend on the switch position function anymore, which results in zero ripple output current. The same holds for x_1 in case of the *inverse matching condition*, $n = k^{-1}$, $\beta = \gamma$, which results in zero ripple input current. A third practically relevant condition can be found for $n = 1$, $0 \leq k < 1$, $\alpha = \beta$, which is denoted as the *balanced ripple reduction*. Both the current ripples can be reduced between 0 and approximately 50%.

Remark: These conditions, unfortunately, are often not easy to acquire in practice, i.e., there will always be a certain 'mismatch' between k and n. We come back to this in the next section. Coupled-inductor extensions can also be applied to the classical Buck, Boost and Buck-Boost converters, but in these cases an extra capacitor is needed to serve as a driven voltage source for the secondary inductor, see e.g. [14].

As shown in [6, 9, 11], the switched EL equations are also closely related to the *average* PWM models. For the Ćuk converter given by the dynamic equations (11) this means that the

state variable x is replaced by the average state z, representing the average inductor currents and capacitor voltages, and the discrete signal u is replaced by the duty ratio function D that takes values in the open interval $]0,1[$. The description of the dynamics as described in words above is given by the following more compact matrix representation

$$\mathcal{A}\dot{z} + D\mathcal{J}_1 z + \mathcal{J}_2 z + \mathcal{R}z = \mathcal{E} \tag{12}$$

where $\mathcal{A}$ is invertible, and where $\mathcal{J}_j = -\mathcal{J}_j^\top$ and its elements are given by $\{-1, 0, 1\}$, for $j = 1, 2$. For the coupled-inductor Ćuk converter we have $\mathcal{E} = [E, 0, 0, 0]^\top$ and

$$\mathcal{A} = \begin{bmatrix} L_1 & 0 & L_m & 0 \\ 0 & C_1 & 0 & 0 \\ L_m & 0 & L_2 & 0 \\ 0 & 0 & 0 & C_2 \end{bmatrix} ; \mathcal{J}_1 = \begin{bmatrix} 0 & -1 & 0 & 0 \\ 1 & 0 & 1 & 0 \\ 0 & -1 & 0 & 0 \\ 0 & 0 & 0 & 0 \end{bmatrix} ;$$

$$\mathcal{R} = \begin{bmatrix} 0 & 0 & 0 & 0 \\ 0 & 0 & 0 & 0 \\ 0 & 0 & 0 & 0 \\ 0 & 0 & 0 & R^{-1} \end{bmatrix} ; \mathcal{J}_2 = \begin{bmatrix} 0 & 1 & 0 & 0 \\ -1 & 0 & 0 & 0 \\ 0 & 0 & 0 & -1 \\ 0 & 0 & 1 & 0 \end{bmatrix} .$$

$\square$

The presented Euler-Lagrange modeling technique for (switching) networks results in the same dynamical models as when the Hamiltonian framework is used, e.g. [2, 5], provided that the same level of ideal physics is assumed. However, the Hamiltonian framework does not introduce the 'semi'-physical intermediate help-variables. In case of two mutually coupled-inductors for example, the magnetic energy is now given by

$$\mathcal{H}(\phi) = \frac{1}{2} \begin{bmatrix} \phi_{L_1} \\ \phi_{L_2} \end{bmatrix}^\top \begin{bmatrix} \beta & -\gamma \\ -\gamma & \alpha \end{bmatrix} \begin{bmatrix} \phi_{L_1} \\ \phi_{L_2} \end{bmatrix} , \tag{13}$$

where α, β and γ are given in (5). Nevertheless, the Lagrangian approach gives us the opportunity to apply the well-known passivity-based control techniques, as presented in [6, 9] for the buck, boost and buck-boost converter, but this time for more general electrical network structures.

4 Zero-Dynamics

In the sequel, we continue with the dynamic PWM model of the converter structures, as can be obtained from the previous section, where we now denote the averaged state space variables by z, and the duty cycle by D. The design of passivity based control for the conventional buck, boost, buck-boost and Ćuk converter can be found in [9, 11], whereas further analysis of the closed loop system is explored in some follow-up work, e.g. [12, 13]. Since we have given a general procedure to build an Euler-Lagrange model for switching networks, we can also generally apply the passivity based control design technique. However, one issue that remains is the choice of the average state variable to be stabilized to a certain value, in order to, possibly indirectly, regulate our average output toward a desired equilibrium value. For the conventional boost, buck-boost and Ćuk converters, it was shown in [9, 11] that the average output voltage could not be directly controlled, due to

the unstable zero-dynamics (i.e., for linear systems this corresponds to zeros in the right half plane, or in other words, undesirable non-minimum phase behaviour), and therefore, had to be indirectly controlled via the average input-current, which exposed stable zero-dynamics.

Example (continued) As in [11], given a desired equilibrium value V_{2_d} for the output voltage, which correspond to a constant value of the duty ratio function $D_c = V_{2_d}/(V_{2_d} - E)$, the *unique* corresponding equilibrium values for the average voltages and currents are

$$I_{1_d} = \frac{V_{2_d}^2}{RE}; \quad I_{2_d} = -\frac{V_{2_d}}{R}; \quad V_{1_d} = E - V_{2_d}. \tag{14}$$

This means that if we want to regulate z_4 toward an equilibrium value V_{2_d} which is known to correspond to a steady state value D_c of the duty ratio function D, then such a regulation can be *indirectly* accomplished by stabilizing one of the other average variables toward the corresponding equilibrium values computed in (14).

Henceforth, for the uncoupled-case ($k = 0$) we know for the Ćuk [11], Boost and Buck-Boost converters [9], that a feasible regulation of the output voltage is only achievable through indirect regulation of the input current. But if $k \neq 0$, does the input current still exhibit stable zero-dynamics under all coupling conditions? From the previous section, we know we have two special cases of interest, $k = n$ and $k = n^{-1}$, both with its related 'mismatches' $0 \leq k < n$, $n < k < 1$ and $0 \leq k < n^{-1}$, $n^{-1} < k < 1$, respectively. $\square$

For the converter structures we consider here, we can bring the system in normal form (see e.g., [3]) for the output y given by the state z_i, which has relative degree r_i, then we obtain the new coordinates, $\xi = [\xi_1, \ldots, \xi_{r_i}]^\top$, and $\eta = [\eta_{r_{i+1}}, \ldots, \eta_N]^\top$, with $[\xi, \eta]^\top = \varphi(z)$, and $\varphi_1 = y, \ldots \varphi_{r_i} = y^{(r_i)}$. For the η coordinates, that are related to the state of the zero-dynamics we obtain

$$\frac{\partial \varphi_i(z)}{\partial z} \mathcal{A}^{-1}\mathcal{J}_1 z = 0, \quad i = r_i + 1, \ldots, N.$$

This implies that at least the total energy, given by

$$\varphi_{r_i+1}(z) = \frac{1}{2}z^\top \mathcal{A}z \tag{15}$$

is part of the zero-dynamics. If we drop the assumption that the generalizing forces are independent of the switch, we can still do the above analysis, but then we have to add to the total energy of (15) an additional term which depends on the voltage source.

Example (continued) If we consider the average input current z_1 as the output, for the matching condition $n = k$, $\alpha = \beta$, and thus that

$$\xi_1 := \varphi_1(z) = z_1,$$

and that the state of the zero-dynamics is going to be determined by

$$\eta_1 := \varphi_2(z) = \frac{1}{2}C_1 z_2^2 + \frac{1}{2}(\beta - \alpha)^{-1}(z_1 + z_3)^2$$
$$\eta_2 := \varphi_3(z) = z_3$$
$$\eta_3 := \varphi_4(z) = z_4.$$

It is seen that the relative degree equals $r_1 = 1$. We then proceed by calculating $z = \varphi^{-1}[\xi, \eta]^\top$, and form the zero-dynamics by giving z_1 its desired value I_{1_d}, i.e., then $\xi_1 = I_{1_d}$, and we consider the dynamics of η, see [3]. In order to determine whether or not the zero-dynamics are stable, we linearize the dynamics at the equilibrium point η^0, that corresponds to (14). In order to numerically compute the eigenvalues, we need to complete the design of our converter first. In the sequel we use the following realistic values [11]: $E = 100V$, $R = 40\Omega$, $C_1 = C_2 = 10\mu F$, and the coupling parameters are set to: $n = 0.7, 0 \le k < 1$, where for the matching condition we take $k = n$, $L_1 = 600\mu H$, $L_2 \propto k$ and for the inverse matching we take $L_2 = 600\mu H$, $L_1 \propto k$. In case for the zero-dynamics of z_1 for the matching condition this yields for the linearization the eigenvalues $(-1655, -2248 \pm 1538.9i)$. We conclude that for this condition z_1 shows stable zero-dynamics.

Next, consider the case that $k = n^{-1}$. In this case the normal form is found as

$$\xi_1 := \varphi_1(z) = z_1,$$
$$\xi_2 := \varphi_2(z) = -\beta z_2 + \beta E - \beta z_4 = \dot{z}_1,$$

and determined the state of the zero-dynamics by

$$\eta_1 := \varphi_3(z) = \tfrac{1}{2}C_1 z_2^2 + \tfrac{1}{2}(\beta - \alpha)^{-1}(z_1 + z_3)^2$$
$$\eta_2 := \varphi_4(z) = z_4.$$

We now notice that the relative degree equals $r_1 = 2$, which tells us that that the order of the zero-dynamics is reduced from 3 to 2. Following the same procedure as above, we calculate the eigenvalues after the linearization as $(-1655, -100850)$. Again, we conclude that the regulation through z_1 remains feasible.

Finally, we consider the (practical) 'mismatch' cases. The general description of the normal form is now given by

$$\xi_1 := \varphi_1(z) = z_1,$$

and that the state of the zero-dynamics is going to be determined by

$$\eta_1 := \varphi_2(z) = \tfrac{1}{2}(\beta - \gamma)^{-1}z_1^2 + \tfrac{1}{2}C_1 z_2^2 + \tfrac{1}{2}(\alpha - \gamma)^{-1}z_3^2$$
$$\eta_2 := \varphi_3(z) = -\tfrac{1}{C_1}z_1 - \tfrac{1}{C_1}z_3$$
$$\eta_3 := \varphi_4(z) = z_4.$$

Again we perform similar calculations as before, but now for all values of k in the closed interval $0 \le k < 1$, except for $k = n$ and $k = n^{-1}$. The calculations are performed using MATLAB, and we find the eigenvalues as a function of k, as depicted in Fig. 3, where 'o' is denoting the corresponding starting points for k. ¿From Fig. 3.(d) we conclude that in case of inverse matching condition 'mismatch' $k > n^{-1}$ all states in the converter show non-minimum phase behaviour. For that, it is *not* possible to apply the passivity-based controller techniques. Fortunately, this range of adjustments will not be of prime concern in a practical situation where we rather choose for zero output current ripple, corresponding to the matching condition instead of the inverse matching condition.
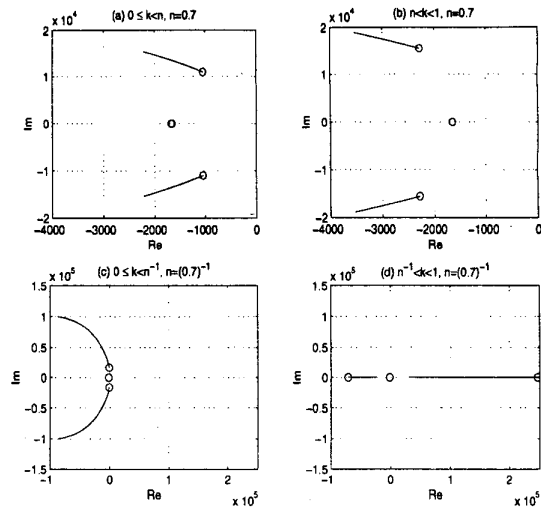

Figure 3: Eigenvalues of the zero-dynamics of the input current for: (a,b) matching-condition mismatches, (c,d) inverse matching-condition mismatches

5 Adaptive Passivity-Based Stabilization of the Zero-Output Ripple Ćuk Converter

We now provide the only feasible regulation based on an *indirect* output capacitor voltage control, achievable through the regulation of the input current. In order to account for parametric uncertainty and changes in load we define the following version of the control reference as

$$z_{1d} = I_{1_d} = \theta \frac{V_{2d}^2}{E}, \tag{16}$$

where the quantity θ denotes the estimate of R^{-1}. Corresponding to this objective for the input current z_1, the required input voltage, output voltage and output current may be represented by the functions $z_{2d}(t)$, $z_{3d}(t)$ and $z_{4d}(t)$, to be determined. Now we follow the procedures as given in [6, 9, 11], and obtain the following *implicit* definition of our controller that preserves passivity of the closed loop:

$$\mathcal{A}\dot{z}_d + D\mathcal{J}_1 z_d + \mathcal{J}_2 z_d + \Theta z_d - \mathcal{R}^i \tilde{z} = \mathcal{E} \tag{17}$$

where $\tilde{z} = z - z_d$, denotes the state *error dynamics*. The necessary damping injection that is required for asymptotic stability is accomplished through $\mathcal{R}^i = \text{diag}[R_1, R_2^{-1}, R_3, R_4^{-1}]$. The estimation matrix is denoted $\Theta = \text{diag}[0, 0, 0, \theta]$, where θ is given by

$$\theta = \theta^0 - \int_0^t z_{2_d} \tilde{z}_4 d\tau. \tag{18}$$

Hence, we find an explicit definition of our controller by choosing the control rule

$$D = \frac{\beta z_{2d} + \gamma z_{4d} - \beta E - \beta R_1 \tilde{z}_1 + \gamma R_3 \tilde{z}_3 - \theta \frac{\dot{V}_{2d}^2}{E}}{(\beta - \gamma)z_{2d}} \tag{19}$$

and let the functional relations z_{2d}, z_{3d}, z_{4d} as in (17). For further analysis, we refer to related considerations and remarks

as given in [6, 9]. The above developments lead to a full-state feedback scheme, which is based on philosophies that can be found in [4, 8].
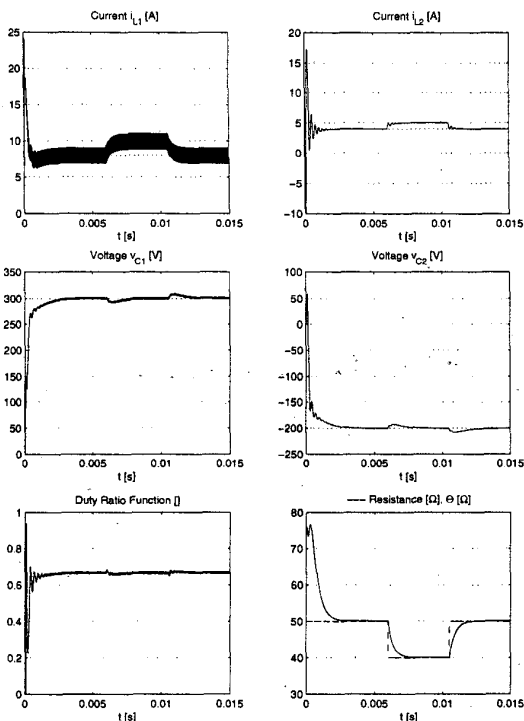

Figure 4: Simulation of the closed-loop passivity-based Ćuk converter with zero-output ripple

In Fig. 4, some simulation results are depicted for the Ćuk converter (11) in closed-loop with the controller (17). The same values, with $k = n$, for the components as in the previous section have been considered for the simulation. To depict the robustness of the controller with respect to abrupt unmodeled changes in the load resistance R, a temporary (step) change in the load resistance of 20% of its nominal value is applied. The control parameters are set to $R_1 = 1$, $R_2 = 2$, $R_3 = 10$ and $R_4 = 15$. The initial conditions of the Ćuk converter where set $x^0 = [0, 0, 0, 0]^\top$, while for the desired control state $z_d^0 = [8, 300, 4, -200]^\top$. As can be seen from the figure, the controller achieves the desired indirect stabilization of the output voltage around the desired equilibrium value. During the sudden change in load, the controller rapidly manages to estimate the (new) value of the load resistance. Notice that the output current ripple equals zero as expected.

6 Conclusions

A method has been presented to build an Euler-Lagrange model for switching electrical networks, which is also applicable to ideal electrical networks without switches. In addition, we have included coupled magnetics into the Lagrangian framework. The method presented here can also be performed for Hamiltonian systems, which is a recent topic of study in e.g., [2, 5].

Future research is recommended towards the involvement of more non-ideal physical effects, a more general statement about the non-minimum phase structure, and the influence of more complex topologies that are given in the power electronics literature. Furthermore, in general it remains a problem to tune the controller in an optimal way, since the corresponding equations are quite complex. It is therefore recommended to search for smart algorithms to tackle this problem. Some preliminary results on this topic can be found in [12, 13].

Acknowledgement

References

[1] S. Ćuk and R.D. Middlebrook, *Coupled-Inductor and Other Extensions of a New Optimum Topology Switching DC-to-DC Converter*, Advances in Switched-Mode Power Conversion, Vol. 2. Pasadena, CA: TESLAco, 331-347, 1981.

[2] G. Escobar, A.J. van der Schaft, R. Ortega, *A Hamiltonian viewpoint in the modeling of switching power converters*, Automatica, Vol. 35 (1999) 445-452.

[3] A. Isidori, *Nonlinear Control Systems*, Third Edition, Springer Verlag, London (1995).

[4] J.G. Kassakian, M. Schlecht and G.C. Verghese, *Principles of power electronics*, Addison-Wesley, Reading, MA (1991).

[5] B. Maschke, R. Ortega, A.J. van der Schaft, *Energy-based Lyapunov functions for forced Hamiltonian systems with dissipation*, to appear in IEEE Trans. Aut. Contr..

[6] R. Ortega, A. Loría, P.J. Nicklasson and H. Sira-Ramírez, *Passivity-Based Control of Euler-Lagrange Systems; Mechanical, Electrical and Electromechanical Applications*, Springer-Verlag London Limited, 1998.

[7] H. Sira-Ramírez, *A geometric approach to pulse-width-modulated control in nonlinear dynamical system*, IEEE Trans. Aut. Contr. AC-34 (1989) 184-187.

[8] H. Sira-Ramírez, P. Lischinsky-Arenas, *Dynamical discontinuous feedback control of nonlinear system*, IEEE Trans. Aut. Contr. AC-35 (1990) 1373-1378.

[9] H. Sira-Ramírez, R.A. Perez-Moreno, R. Ortega, M. Garcia-Esteban, *Passivity-Based Controllers for the Stabilization of DC-to-DC Power Converters*, Automatica, Vol.33, 4 (1997) 499-513.

[10] A.J. van der Schaft, *$\mathcal{L}_2$-gain and passivity techniques in nonlinear control*, Springer Verlag, Lecture Notes in Contr. & Inf. Sc. 218, 1996.

[11] J.M.A. Scherpen, J.B. Klaassens and L. Ballini, *Lagrangian Modeling and Control of DC-to-DC Converters*, IEEE INTELEC Copenhagen, June 1999, 99CH37007, Nr. 31-41.

[12] J.M.A. Scherpen, R. Ortega, *On nonlinear control of Euler-Lagrange system: Disturbance attenuation properties*, System & Control Letters 30,pp.49-56, 1997.

[13] J.M.A. Scherpen, R. Ortega, G. Escobar, *On disturbance attenuation properties of control schemes for Euler-Lagrange systems: theoretical and experimental results*, Proc. Eur. Contr. Conf. Brussels, Vol. 6a, FR-A A6, 6pp., (July 1997).

[14] J. Wang, W.G. Dunford and K. Maunch, *Analysis of a Ripple-Free Input-Current Boost Converter with Discontinuous Conduction Characteristics*, IEEE Power Electronics, Vol. 12, No. 4, July 1997.